

## ORIGINAL RESEARCH ARTICLE

# The different erosion fate of the headland-embayed beaches on the muddy and sandy coasts of China

Abiola John Osanyintuyi<sup>1</sup>, Yong-Hong Wang<sup>1,2,\*</sup>, Yiheng Huang<sup>1</sup>, Saddam Aliyu<sup>1</sup>, Nor Aieni Haji Mokhtar<sup>3</sup>

<sup>1</sup> Key Lab of Submarine Geosciences and Prospecting Techniques, MOE and College of Marine Geosciences, Ocean University of China, Qingdao 266100, Shandong Province, China

<sup>2</sup> Laboratory of Marine Geology and Environment, Qingdao National Laboratory for Marine Science and Technology, Qingdao 266237, Shandong Province, China

<sup>3</sup> Institute of Oceanography and Environment, University Malaysia Terengganu, Kuala Terengganu 21300, Malaysia

\* Corresponding author: Wang Yong-Hong, yonghongw@ouc.edu.cn

## ABSTRACT

China's beaches exhibit different geomorphic characteristics depending on location. Due to increasing contemporary climate change, induced storm activities and human activities, beaches along the Chinese coast have been exposed to the risk of erosion. This article examines the different shoreline evolution processes from 1973 to 2021 as well as the erosion vulnerability of 9 headland-embayed beaches (of which 5 beaches, each at Baishawan, Dasha, Dongdan, Nanshajiao, and Mushao are on the muddy coast in Southern China and 4 beaches, namely, Bathing Beach 1, 2, 3 and Shilaoren Beach are on the sandy coast in Northern China) based on the inherent geomorphic characteristics and nearshore hydroclimatic factors of the beaches. In the analysis, there were 3 stages. During the first stage, erosion dominated both the muddy and sandy coasts as a result of intense storm conditions. During the second stage, the beaches had earlier recovered as a function of natural processes, however, storm activities later eroded the beaches. During the third stage, most of the beaches accreted as a result of coastal engineering interventions and beach nourishment project. The shoreline analysis results indicate that beaches on the muddy and sandy coasts have been eroding in the long term. During the first erosion stage, erosion is more severe on the muddy coast than on the sandy coast in the short term. On the sandy coast, the beaches recorded severe erosion from 1973 to 1998. Of the 9 beaches, the most eroded location was at Dasha on the muddy coast (LRR:  $-5.315$  m/y; EPR:  $-5.671$  m/y; NSM:  $-141.94$  m) between 1974 and 1998. In summary, beaches on muddy coasts are more vulnerable to erosion than those on sandy coasts. On the muddy coast, there has been a shortage in the supply of sediment from the Yangtze River-derived sediment to the coast. The primary source of sand material for the studied beaches on the muddy coast has been the regular storm condition that changes the sand-mud transition line on the coast. For the sandy beaches, the primary factor responsible for the vulnerability and beach modification includes a shortage in the natural supply of beach material and storm activities, however, recent beach nourishment and coastal protection procedures are gradually stabilizing the beaches. Ultimately, the outcome of this research is suitable for beach management procedures on the Chinese coast.

**Keywords:** China coast; storm surge erosion; Zhejiang sandy beach; Qingdao shoreline; sand mud transition

## ARTICLE INFO

Received: 7 August 2023  
Accepted: 19 September 2023  
Available online: 28 September 2023

## COPYRIGHT

Copyright © 2023 by author(s).  
Marine and Environment is published by  
EnPress Publisher LLC. This work is licensed  
under the Creative Commons Attribution-  
NonCommercial 4.0 International License  
(CC BY-NC 4.0).  
<https://creativecommons.org/licenses/by-nc/4.0/>

## 1. Introduction

Beaches are important and fragile locations that are affected by both human and natural factors. They are vulnerable to human-induced interventions that affect the dynamics of sediment on the beach such as beach sand mining, sand nourishments, and nearshore soft and hard engineering structures<sup>[1,2]</sup>. Naturally, beaches are dynamic environments, they are controlled principally by complex factors including wave energy, tides, storm surges, and sediment grain size<sup>[3-5]</sup>. The contemporary global climate change, particularly, increased storm frequency and sea-level rise, has added a new dimension to

worldwide modifications of sandy shorelines<sup>[5]</sup>. The vulnerability of beaches to human actions and concomitant climate change is exacerbated when they are low-lying and characterized by a natural supply of beach material<sup>[6,7]</sup>.

Around the world, beaches have been eroding at an alarming rate. For example, in Nigeria<sup>[8]</sup>, Spain<sup>[3]</sup>, United Kingdom and France<sup>[4]</sup>, Sri Lanka<sup>[9]</sup> as well as China<sup>[1,10-12]</sup>. The factors responsible for the changes on the beaches could vary with sedimentary and geomorphological characteristics. Usually, compared with sandy beaches, muddy beaches are more vulnerable to these factors<sup>[13]</sup>.

Along the Chinese coast, the geology condition, human interaction, and natural factors on beaches vary with location. The subsidence belts such as the Yellow River and Yangtze River estuaries are muddy coastal locations marked with reduced sediment supply due to large human modifications such as the construction of the Three Gorges Dam along the Yangtze River<sup>[2,10,14]</sup>. The uplift belts, for example, the Shandong Province and Xiamen Island coasts are characterized by sandy coastal environments that have received numerous beach reclamation and experiencing erosion as a result of storm surges and hurricanes, and sand mining<sup>[1,10]</sup>. The Northern coast of China such as Qingdao is marked with rocky headland and sandy cape-bay beaches. In the South, as in the Zhejiang region, the coast is marked by muddy tidal flats often characterized by small sandy beaches.

Except Zhejiang, China, the presence of “small” sandy beaches in muddy coastal environments has been reported in several locations worldwide. Of all, the coastal stretch between Orinoco River, Maroni River, and Amazon River estuaries in South America host good examples of sandy beaches in a muddy coastal environment. The large fine sediment discharge from the rivers, longshore current, and wave characteristics have created small embayed sandy pockets in Yalimapo, French Guiana<sup>[15]</sup>, and Cayenne, French Guiana<sup>[16,17]</sup>. The condition is facilitated by complex interactions between different factors such as the source of sediment supply to the coast, longshore current direction and intensity, nearshore wave energy, storm conditions as well as ocean currents<sup>[15-18]</sup>.

Similarly, rocky headland and sandy embayed beaches such as those in Zhejiang and Qingdao, China are common around the world. In fact, about 50% of the world’s embayed beaches are located on naturally occurring or human-engineered headlands<sup>[19,20]</sup>. For example, in Narrabeen-Collaroy embayment, Sydney, Australia<sup>[21]</sup>, Haeundae Beach, Korea<sup>[22]</sup>, beaches on New South Wales coast, Australia<sup>[23]</sup> and several beaches in the Mediterranean coasts of Italy, France, Spain, Tunisia and Turkey<sup>[20]</sup>. The morphological conditions of these embayed sandy beaches on rocky headlands are controlled by nearshore wave interaction, sediment supply from catchment sources, and the storm climate along the coasts<sup>[19-23]</sup>.

The presence of Sandy beaches is facilitated by the geomorphic conditions of beaches around the muddy coastal environment. For example, embayed beaches are dominated by a closed sediment circulation system. Regardless of negligible residual transport, embayed beaches are affected by cross-shore and long-shore sediment transport processes<sup>[22]</sup>.

Meanwhile, vulnerability assessment is an important indicator for evaluating coastal erosion<sup>[1]</sup>. Besides, identifying factors that cause beach erosion is important in beach management. The vulnerability of sandy beaches to erosion is culminated by the inherent and external characteristics and factors acting on the beach, including beach material composition, geology, beach profile, sea level, the shape of the beach, and storm activities on the beach<sup>[24-28]</sup>. Studies accessing the long-term and short-term changes and vulnerabilities of sandy beaches have employed several methods of analysis including geophysical observation and analysis<sup>[7,18]</sup>, computer modeling<sup>[1,4,5,29]</sup>, geochronology<sup>[30]</sup> and satellite images<sup>[8,9,11]</sup>.

Several studies have attempted to define the vulnerability and as well, describe the contributing factors of Mainland China to erosion<sup>[1,2,5,7,10-12,14,18,29,30]</sup>. However, most of these studies have focused specifically on

large-scale (entire Chinese coast) and regional (sections of the Chinese coast with the same geological characteristics and nearshore dynamics). Regardless, there is a need to compare and contrast the vulnerability of Chinese beaches with different geomorphological and inherent geological characteristics. Moreover, there is a need to understand the evolution of sandy *beach pockets* found in sandy, muddy and rocky *coastal environments* around the world.

Hence, in an attempt to quantify the vulnerability, as well as better understand the implications of human and natural factors affecting the sandy beaches on the Chinese coast, this paper utilizes field survey, remote sensing, and comprehensive analysis to study the shoreline change characteristics and vulnerability of 9 embayed beaches on two regions with different geological characteristics and nearshore dynamics along the coast of Chinese mainland. Five (5) of the beaches are located along the coast of Zhejiang province of China (Southern part of China). Four (4) of the beaches are located on the Qingdao coast of Shandong province, China (Northern part of China). The objective of this research hence is to (1) describe the short-term and long-term characteristics of the shoreline morpho-dynamics. (2) Indicate the vulnerability level using each beach's geomorphic and nearshore hydrodynamic conditions. (3) Compare and contrast the factors responsible for the changes observed on the beaches studied using a comprehensive proxy analysis method. The outcome of this analysis will provide additional information to the existing repository on the effect of anthropogenic and storm-induced erosion on the beaches along the Chinese coast. In addition, the result of this research is suitable for improving the beach management strategies of China. Ultimately, this work will provide clear understanding on the formation of sandy beaches on sandy, rocky and muddy coastal environments around the world.

## 2. Study areas

In this work, five (5) sandy beaches namely Baishawan, Dasha, Dongdan, Mushao, and Nanshajiao were studied in the muddy coast in the Zhejiang province, which are located in southern China (**Figure 1(a)**). Four (4) sandy beaches were studied in Qingdao, China namely Bathing Beach 1, Bathing Beach 2, Bathing Beach 3, and Shilaoren (**Figure 1(b)**).

For the sake of the scope of this article, Baishawan, Dasha, Dongdan, Mushao, and Nanshajiao, sandy beaches located in a mud dominated coast near Samen Bay area of Zhejiang province in China would be referred to as “muddy coast beaches” while Bathing Beach 1, Bathing Beach 2, Bathing Beach 3, and Shilaoren, sandy beaches located in sand and rock dominated Qingdao, Shandong, China would be referred to as “sandy coast beaches” in this article.

### 2.1. Beaches in the muddy coast (Zhejiang Province)

Although the studied beaches in this region are sandy (**Figure 1(a)**), the coastal types of Zhejiang Province could be generalized into the muddy (about 50% of total length), bedrock (40%), and sand coast (4%)<sup>[7]</sup>. The coast has embayed beaches with a wide and flat coastal shelf open to the marginal sea. The beaches are directly exposed to the East China Sea and have undulating topography<sup>[14,31]</sup>. Under the influence of the hydrodynamic condition and sediment source, these coasts have obvious seasonal variations: erosion in summer and deposition in winter<sup>[7,31]</sup>.

Here, the East Asian monsoon is the dominant physical driver of the formation, distribution, and sedimentary processes of the mud belt<sup>[2]</sup>. The main tidal characteristics are mixed semidiurnal tides with medium tide ranges and high current velocities<sup>[7]</sup>. During summer, the Yangtze River discharges large amounts of water and sediments with 32% of the riverine sediment load estimated to be deposited at the river mouth sites during this time. During winter, intensified East Asian Monsoon activities and wave action resuspend the deposits of river-derived sediment in the mud area<sup>[2]</sup>.

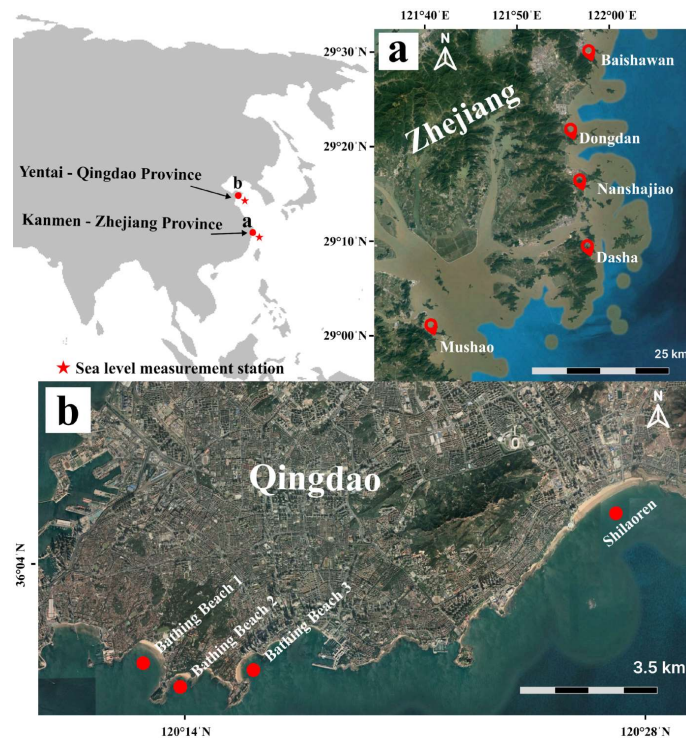


**Figure 1.** The 9 studied sandy embayed beaches on headlands are located along the China Mainland coast. **(a)** Five of the beaches (Baishawan, Dasha, Dongdan, Mushao, and Nanshajiao) are located in the mud dominated coast of Zhejiang, Southern part of China; **(b)** Four of the beaches (Bathing Beach 1, Bathing Beach 2, Bathing Beach 3, and Shilaoren) are located in the sandy coast of Qingdao, Northern part of China. The red stars indicated the location of the sea level data measurement station in Kanmen (Zhejiang) and Yantai (Qingdao).

The general current circulation system here is dominated by the Taiwan Warm Current (TWC). The flood currents come from the outer shelf and flow toward the nearshore area, while the ebb currents have the opposite behavior<sup>[7]</sup>. The winter monsoon also drives the Taiwan Warm Current (TWC) to form upwelling circulation offshore, with the Zhejiang–Fujian Coast Current (ZFCC) causing downwelling in the near-shore region. Upwelling and downwelling circulation constrains the distribution of fine-grained sediments within the inner shelf (<75 m isobath) and formed the “inner shelf mud area of the East China Sea”. In addition, the circulation prevents sediments from escaping to deeper waters in the East China Sea, hence favoring fine-grain sediments to cover the relict sand located on the middle and outer shelves<sup>[2,7]</sup>.

Here, surge waves are more frequent than wind waves affected by southeasterly winds<sup>[7]</sup>. The dominating strong Eastward wave conditions are stronger in autumn due to the frequent storm (including typhoons and storm surges) conditions during the period<sup>[32]</sup>. The location is also one of the regions that are most affected by storm activities along the Chinese coast. The sea level rise regime along this area in the recent few decades has risen as high as 6.6 mm/year<sup>[10]</sup>.

## 2.2. Beaches on the sandy coast (Qingdao Province)

Qingdao is located in the southeastern part of Shandong Peninsula, China. It is bordered by the Yellow Sea in the East and South, Yantai City in the Northeast, Rizhao City in the Southwest, and Weifang City in the West. Qingdao coast has flat beaches that are made of rocky and coarse sandy clastic materials with cliffy beakheads distributed over sections of the study area<sup>[6]</sup>. The beaches here are located at the edge of the Yellow Sea and are characterized by high wind wave energy that interchange the beach materials with sediments in adjoining bays<sup>[5,6]</sup>.

The wave and wind characteristics here change with the season. The annual mean wave height is 0.7 m. Qingdao’s wave height increases gradually in the first half of the year and reaches a maximum of 0.9 m in

July. In the second half of the year, the wave height decreases gradually to a minimum of 0.5 m in January and December. In winter, the waves are usually in the NWW-NNW direction, with 18% in NW, and 7% NNW; in spring the wind waves are in E (14%) and SEE (9%); in summer, the main wind direction is ES, and 12% are in E and 9% in SEE, and in fall the frequency of NW wave is 10%<sup>[6]</sup>.

Qingdao's tidal regime type is characterized by regular semi-diurnal tides, with an average tidal range of 2.8 m and a spring tidal range of 4.75 m<sup>[5,6]</sup>. The sea level rise characteristics along this area in the recent few decades have been up to 4.8 mm/year<sup>[10]</sup>. The storm condition along the coast is not as frequent when compared to Zhejiang (for the sake of this study), however, the coast is still affected by temperate and tropical storm surges such as typhoons. During the storm surge, semi-open bays facing the open sea (as in the studied beaches) are vulnerable to the attack of rough waves.

The coast of Qingdao is marked with bays that were formed during the Holocene transgression<sup>[5]</sup>. The rock in Qingdao bays is mainly Mesozoic granite and some volcanic assemblages. There is a breccia tuff and volcanic silication zone outcrop near Shilaoren. Faults are mainly developed in NE-NNE as the controlling factor over the structural and geomorphological patterns here.

### 3. Data and methodology

#### 3.1. Shoreline change

Landsat imagery is widely used for shoreline change analysis along sandy beaches around the world. They have spatial, spectral, and radiometric characteristics as well as temporal continuity that make them suitable for implementation in shoreline change analysis of low-lying sandy beaches<sup>[8,11]</sup>.

Cloud-free multitemporal Landsat MSS, TM, ETM+, and OLI images from 1973 to 2021 with pixel resolution of 30 m were downloaded from the USGS Global Visualization Viewer repository<sup>[33]</sup>. Storm conditions are more frequent along the Chinese coast between July and September<sup>[5,34]</sup>, hence we avoided selecting satellite images during this period. **Table 1** shows a comprehensive detail of the respective Landsat images used in both study areas considered in this research.

**Table 1.** Details of the multitemporal Landsat imageries used for the shoreline position identification along the studied Zhejiang and Qingdao beaches.

Headland-embayed beaches in the muddy coast (Zhejiang)		Headland-embayed beaches in the Sandy coast (Qingdao)	
Sensor	Date	Sensor	Date
Landsat 1/MSS	01/30/1973	Landsat 1/MSS	05/02/1975
Landsat 1/MSS	01/08/1983	Landsat 1/MSS	02/02/1980
Landsat 1/MSS	01/07/1986	Landsat 1/MSS	11/04/1986
Landsat 1/MSS	02/22/1991	N/A	N/A
Landsat 5/TM	02/09/1998	Landsat 5/TM	01/11/1998
Landsat 5/TM	02/20/2002	Landsat 5/TM	01/28/2001
Landsat 5/TM	04/07/2007	Landsat 5/TM	04/02/2006
Landsat 7/ETM+	01/12/2011	Landsat 7/ETM+	01/26/2011
Landsat 7/ETM+	01/03/2015	Landsat 7/ETM+	03/28/2016
Landsat 8/OLI	01/18/2019	Landsat 8/OLI	02/22/2021

Considering the small scale of the studied beaches, we employed semi-automatic shoreline identification to elucidate the regression and progradation history of the shoreline position of the studied beaches. We use image filtering and arithmetic operations to digitize the shoreline on the high-water mark before manual corrections. The shoreline change rates were calculated in the form of three statistical methods namely LRR, EPR, and NSM using the Digital Shoreline Analysis System (DSAS) plugin on ArcGIS 10.8.

We selected alternating years for the two study areas according to the satellite images available suitable for delineating the shoreline position through the semi-automated water-line identification method.

### 3.2. Beach vulnerability assessment

The vulnerability of a beach to erosion is affected by the local geomorphological characteristics of the beach and its nearshore characteristics<sup>[24,25,27]</sup>. The choice of the indicators considered in this study is affected by the availability of reliable data to assess the vulnerability of the selected study area.

After identifying the indicators and assigning a weighting value for each one, the beach vulnerability can be determined from the average of the indicator for each variable<sup>[24,25,35,36]</sup>. The resulting value which indicates the beach vulnerability for each of the beaches was distributed in three classes, with respectively associated vulnerabilities of low, moderate, and high (**Table 2**).

The weighing values were determined from field survey and comprehensive analysis of the factors that are responsible for the changes in the beach geomorphology. For example, beaches whose local geological characteristics can be easily eroded (for instance, loose sand) are more susceptible to erosion than those that are not easily eroded (e.g., rock basement). Hence a higher weighting classification level would be assigned to sandy beaches compared to rocky beaches when measuring their vulnerability to erosion.

**Table 2** shows the weighting values for each variable considered in the vulnerability assessment for this work. The weights of each variable were distributed within the range of 0 to 3, where values that tend towards 0 represent low vulnerability and values that tend towards 3 represent high vulnerability.

The main variables considered for the vulnerability of the studied beaches are (1) long-term shoreline variation over the period of 1973 to 2019 for Zhejiang beaches and 1975 to 2021 for Qingdao beaches. This variable was considered because the change rate of a shoreline, in connection with the geomorphology of a beach, indicates its response of the beach to factors that influence it, and as well, affect the vulnerability of a beach to erosion<sup>[25,26]</sup>; (2) the frequency of storm activities on the beaches 1991 to 2021. The variable was incorporated into the vulnerability analysis because the frequency of storm activities on a beach affects its geomorphology<sup>[26,35]</sup>; (3) summary of the sea level from 1980 to 2021, adapted from the China Sea Level Bulletin<sup>[37]</sup>. Sea level data was considered here because the intensity of sea level rise on a beach affects the storm conditions observed on the beach<sup>[5,36,38]</sup>; (4) the geology of each beach, described by the distribution of sand, silt and bedrock characteristics of each beach. According to Ding et al.<sup>[26]</sup>, beach geology plays an important role in the level of vulnerability of a beach. Data acquired from field survey, remote sensing, and comprehensive literature review; (5) the beach protection of each beach. Which describes the embayment of each beach. This research included beach protection because erosion-preventing facilities available on a beach will affect the vulnerability of a beach<sup>[35]</sup>. Data was acquired from field surveys and remote sensing.

**Table 2.** List of the variables considered, their source, years of data incorporated and vulnerability weight classification of the variables used in the vulnerability assessment. NA indicates Not Applicable.

Variable	Data source	Year	Vulnerability weight classification		
			1	2	3
Shoreline change LRR (m/y)	Satellite image analysis	1973–2019 (for Zhejiang); 1975–2021 (for Qingdao)	<-0.15	-0.15 ≤ -1.10 ≥ -1.50	>-1.50
Storm frequency	China Marine Disaster Bulletin	1991–2021	2–For Zhejiang 1–For Qingdao		
Sea level	China Sea Level Bulletin	1980–2021	1 (average change of 3–4 mm/y for all beaches)		
Geology	Field survey and comprehensive analysis	NA	Rocky beach on rocky coast	Sandy beach on sandy coast	Sandy beaches in muddy coast
Beach protection	Field survey and comprehensive analysis	NA	Seawall, natural headland and embayed	Natural headland and embayed	Embayed
Beach vulnerability index			Low vulnerability	Moderate vulnerability	High vulnerability

The beach vulnerability index for Zhejiang and Qingdao beaches is defined thus.

$$BVI = \frac{SC + ST + SL + GE + BP}{5}$$

where, *SC* is the shoreline change, *ST* is the storm frequency on the beach, *SL* is the Sea Level of the beach, *GE* describes the local geology of the beach, *BP* defines the level of man-made beach protection against erosion on the beach, and *BVI* is beach vulnerability index.

## 4. Result

### 4.1. Shoreline change

The summary of the shoreline change rates and respective information of the stages and statistical methods are displayed in **Table 3**. The results show varying short-term and long-term changes in terms of erosion as well as accretion.

#### 4.1.1. Shoreline changes on three stages

For the first stage, we considered shoreline positions of the years 1973, 1983, 1986, 1991, and 1998 for sandy beaches studied in Zhejiang and the years 1975, 1980, 1986, and 1998 for beaches in Qingdao. For the second stage, we considered shoreline position in the years 1998, 2002, 2007, 2011, and 2015 for Zhejiang beaches and shoreline position in the years 2001, 2006, and 2011 for Qingdao beaches. During the third stage, we considered shoreline positions in 2015 and 2019 (for Zhejiang beaches) and 2011, 2016, and 2021 (for Qingdao beaches) for the analysis.

##### The first stage

For the first stage (1973/1975 to 1998—Zhejiang and Qingdao beaches respectively), all the beaches showed a continuous landward shift in the shoreline positions during this stage (**Figures 2 and 3**). In 1998, the situation intensified as the shoreline position shifted farthest inland. For example, in Bathing Beach 2, most of the beach area was drowned (**Figure 2(b)**). We traced the inundation during this stage to several typhoon storm conditions that were recorded before 1998.

##### The second stage

The studied beaches experienced a series of fluctuations during this stage (**Figures 2 and 3**). Initially, all the beaches had recovered and shifted seaward from the retreat experienced in 1998, however, they later experienced recurrent seaward and landward fluctuation that ended with a landward movement in 2015 (for Zhejiang beaches) and 2011 (for Qingdao beaches). The frequent storm conditions on these beaches were suspected to be responsible for beach loss during this stage.

##### The third stage

During this stage, all the beaches showed a positive budget compared to respective previous years (**Figures 2 and 3**). It is admitted that the beach management procedure and protective features have improved compared to previous stages in some of the studied beaches. For example, at Bathing Beach 2, the beach was protected by breakwaters perpendicular to the beach and created a relatively enclosed system due to the curvature of the beach, hence preventing the erosion of the coast by natural nearshore dynamics including waves, and storm conditions. This later contributed to the positive budget recorded on the beach in our long-term analysis (**Figure 2(b)**).

#### 4.1.2. Long term and short-term changes

In this section of the paper, we highlighted the results of the long-term and short-term shoreline evolution of selected sandy beaches in Zhejiang and Qingdao, China. For the analysis, we divided the results into 3

different short-term periods (For Zhejiang beaches; 1973–1998; 1998–2015; 2015–2019, For Qingdao beaches; 1975–1998; 1998–2011; 2011–2021) as a function of a literature review and comprehensive analysis of the conditions of the coasts and recorded results.

For the long-term analysis, we considered all the shoreline positions on respective study areas (i.e., 1973, 1983, 1986, 1991, 1998, 2002, 2007, 2011, 2015, and 2019 for Zhejiang beaches and 1975, 1980, 1986, 1999, 2001, 2006, 2011, 2016 and 2021 for Qingdao beaches).

The short-term results showed a similar trend of change in both locations, marked by near-stable beaches with fluctuating trends in accretion and erosion in recent years and severely eroded beaches before 2000 (**Figures 2 and 3**). In the long term, the analysis indicates a retreating coastline in both regions shows an overall similar trend in the movement and coinciding offshore and landward movement of this shoreline position during respective years on these beaches.

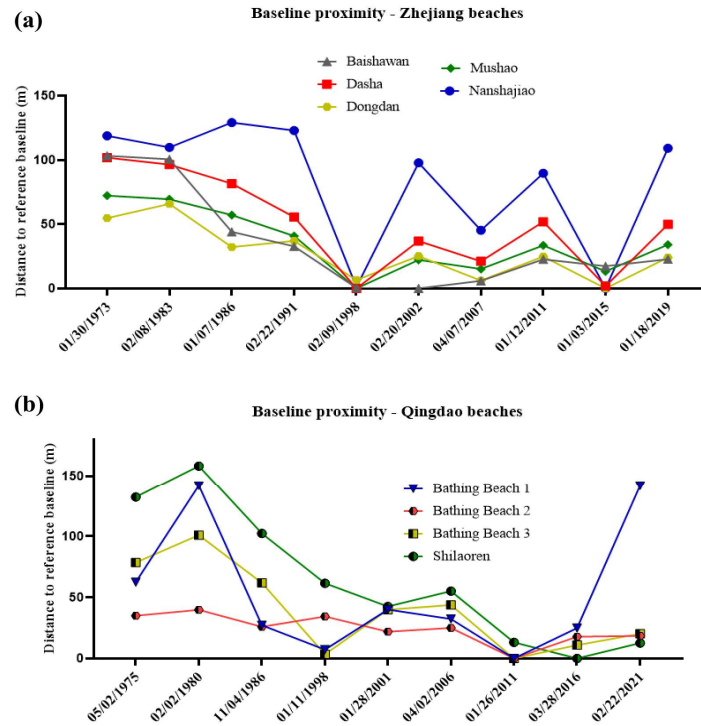
NSM, expressed in m herein, is the total distance between the earliest and most recent shorelines for each transect. EPR, expressed in m/y herein, is calculated by dividing the NSM by the number of years between the oldest and the most recent shoreline. LLR, expressed in m/y herein, is determined by LRR and is computed by fitting a least-squares regression line to multiple shoreline positions for a particular transect.

**Table 3.** The locations with zero change rates and zero shoreline movement indicate a steady shoreline. The LRR analysis result for Zhejiang beaches is not available because we only considered the shoreline position for two years, 2015 and 2019, hence LRR analysis is not possible because it requires at least 3 years of the position of the shorelines. (N/A: Not available).

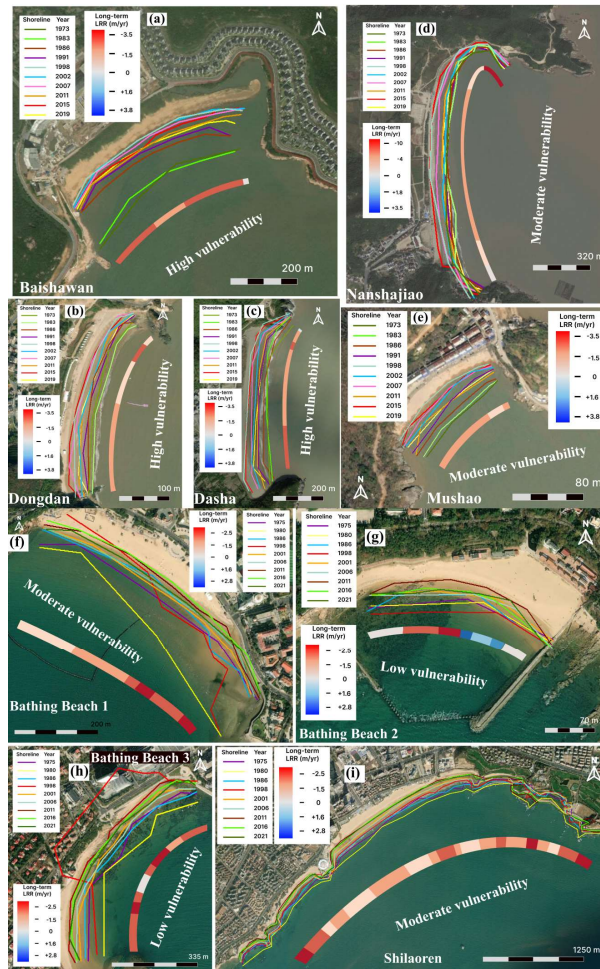
<b>LRR (m/y)</b>								
<b>Beaches on muddy coast</b>	<b>1973–1998</b>		<b>1998–2015</b>		<b>2015–2019</b>		<b>1973–2019</b>	
	<b>Accretion (%)</b>	<b>Erosion (%)</b>						
Baishawan	+0.00 (0%)	-4.847 (100%)	+1.046 (91%)	-0.330 (9%)	N/A	N/A	+0.00 (0%)	-2.138 (100%)
Dongdan	+0.00 (0%)	-1.921 (100%)	+0.201 (23%)	-0.675 (77%)	N/A	N/A	+0.00 (0%)	-0.810 (100%)
Nanshajiao	+2.706 (3%)	-2.825 (97%)	+2.983 (23%)	-2.091 (77%)	N/A	N/A	+0.00 (0%)	-1.321 (100%)
Dasha	+0.00 (0%)	-5.315 (100%)	+2.248 (100%)	-0.00 (0%)	N/A	N/A	+0.00 (0%)	-1.788 (100%)
Mushao	+0.00 (0%)	-2.936 (100%)	+0.818 (100%)	-0.00 (0%)	N/A	N/A	+0.00 (0%)	-1.021 (100%)

<b>LRR (m/y)</b>								
<b>Beaches on sandy coast</b>	<b>1975–1998</b>		<b>1998–2011</b>		<b>2011–2021</b>		<b>1975–2021</b>	
	<b>Accretion (%)</b>	<b>Erosion (%)</b>						
Bathing 1	-0.0988 (100%)	-0.00 (0%)	+1.078 (18%)	-3.534 (82%)	+1.586 (75%)	-1.523 (25%)	+0.00 (0%)	-0.117 (100%)
Bathing 2	+0.010 (100%)	-0.00 (0%)	+0.00 (0%)	-2.838 (100%)	+1.424 (100%)	-0.00 (0%)	+0.00 (50%)	-0.010 (50%)
Bathing 3	+0.00 (0%)	-0.078 (100%)	+5.989 (66%)	-6.591 (34%)	+1.839 (95%)	-0.793 (5%)	+0.00 (0%)	-0.087 (100%)
Shilaoren	+0.00 (0%)	-0.079 (100%)	+9.338 (14%)	-5.198 (86%)	+1.716 (70%)	-0.839 (30%)	+0.00 (0%)	-0.110 (100%)



**Figure 2.** The shifting of the shoreline positions of each beach with respect to a reference to the baseline buffer point. **(a)** Zhejiang beaches; **(b)** Qingdao beaches.



**Figure 3.** The shoreline position of all the years considered in this study on respective beaches. The LRR (long-term analysis considering all the shoreline positions for each beach) results are shown in respective study locations.

## The short-term shoreline changes and summary

All the beaches in the two study locations had a retrograding shoreline for the first stage from 1973/1975 (Zhejiang and Qingdao beaches respectively) to 1998 (**Figures 2 and 3; Table 3**). The shoreline positions were consistent on all the beaches for the years considered in this stage. Initially, in 1983 (for beaches in Zhejiang) and 1980 (for beaches in Qingdao), the shoreline positions had moved seaward, however, there was a recorded retreat of the shorelines in 1998 (**Figure 2**). The LRR, EPR, and NSM statistical analysis showed a negative average for all the beaches during this stage. The lowest value (most eroded locally) was recorded at Dasha (LRR:  $-5.315$  m/y; EPR:  $-5.671$  m/y; NSM:  $-141.94$  m), while the least erosion was recorded at Bathing Beach 2 (LRR:  $-0.00$  m/y; EPR:  $-0.010$  m/y; NSM:  $-2.96$  m). In general, the summary indicates a steady shoreline before 1980, before a sharp retreat that started in early 1980 through to the late 1990s.

The second stage is characterized by fluctuating shoreline positions in both study areas. The shoreline position in 1998 and 2015 (for Zhejiang beaches) was almost the same. The situation was similar in Qingdao beaches for this stage (1998–2011), except for Bathing Beach 2 where the shoreline position shifted farther inland in 2011. However, there was a significant shift in the position of the shorelines in 2002/2001, and 2007/2006 for Zhejiang and Qingdao beaches respectively. In Bathing Beach 3, the recorded inundation in 1998 had recovered in 2011.

During this stage, the shoreline position was the most stable compared to the other two stages. The shoreline position on Zhejiang beaches shifted seaward in 2021 from its initial position in 2015. However, on Qingdao beaches, the shoreline was almost the same in 2011 and 2019.

## The long-term shoreline changes and summary

The result for the long term considered all the shoreline positions for the LRR analysis for both study areas and 1973/1975 and 2019/2021 for Zhejiang and Qingdao beaches respectively for the EPR and NSM analysis. Overall, erosion dominates all the beaches in the long term (**Figures 2 and 3; Table 3**). The analysis indicates that Zhejiang beaches have been severely eroded irrespective of the recorded short-term results. On Qingdao beaches, the situation is similar, but the long-term intensity of erosion is not as high as that on Zhejiang beaches. In fact, at the least eroded beach, Bathing Beach 2, we recorded an accretion in half of the beach in the long term, elsewhere, erosion dominates. The highest level of erosion was at Baishawan with an LRR erosion rate of  $-2.138$  m/y.

## 4.2. Features on hydrodynamics

### 4.2.1. Sea level change

The sea level data was extrapolated from the *China Sea Level Bulletin*<sup>[37]</sup>. For this article, we selected the sea level data from Kanmen (Zhejiang) and Yantai (Qingdao) stations. The location of the stations is marked with a red star in **Figure 1**. According to the *China Sea Level Bulletin*, the average sea level change rate for both study regions is 3–4 mm/y. **Figure 4** shows the trend of sea level change for the two regions from 1980 to 2021.

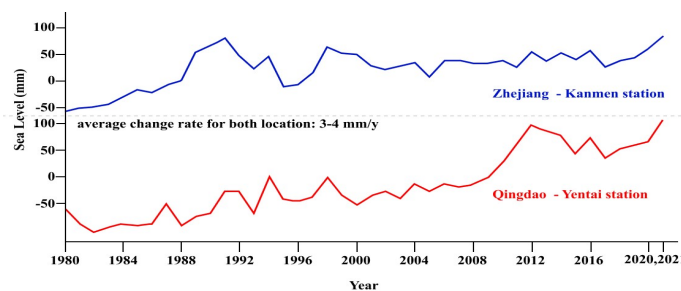


**Figure 4.** The sea level for Zhejiang (Kanmen) and Qingdao (Qingdao) stations from 1980 to 2021. The average change rate for both location is 3–4 mm/y<sup>[37]</sup>.

### 4.2.2. Storm surge

Chinese beaches in the southern part of China (as in Zhejiang) are frequently affected by storm conditions more than the Northern part (as in Qingdao). In **Figure 5**, we presented a summary and frequency of storm surge events in both studied regions. The data presented in this section is the storm surge and typhoon conditions that had landfall connections at Zhejiang and Qingdao provinces, rather than the studied beaches. The summary of storm and typhoon events in China from 1988 to 2021 has been presented in the *China Marine Disaster Bulletin* by the Ministry of Natural Resources, PRC<sup>[39]</sup>.

Zhejiang is one of the locations that is frequently affected by storm surges and typhoons in China. Over the years, the region has experienced some major storm events including the disastrous Typhoon Winne and Polly of 1978 and 1992 respectively. Qingdao is also frequently affected by storm conditions; however, the frequency and intensity of the storm conditions are lesser when compared to Zhejiang<sup>[39]</sup>.

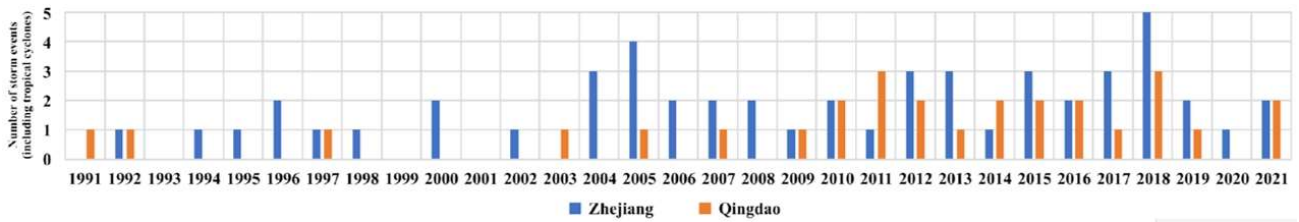


**Figure 5.** The number of storm surge activities including Typhoons that made landfall along the coast of Zhejiang and Qingdao between 1991 and 2021<sup>[39]</sup>.

### 4.2.3. Erosion vulnerability assessment

In general, beaches in Zhejiang indicate more vulnerability to erosion than those in Qingdao when considering the geomorphic and hydrodynamical conditions of the beaches. Of all, Dasha in Zhejiang shows the highest vulnerability while Bathing Beach 2 in Qingdao is the least vulnerable of all the studied beaches. **Table 4** shows the vulnerability level of each beach.

**Table 4.** The level of vulnerability on Zhejiang and Qingdao beaches.

Location	Beach	Vulnerability
Zhejiang	Baishawan	High
	Dongdan	High
	Nanshajiao	Moderate
	Dasha	High
	Mushao	Moderate
Qingdao	Bathing Beach 1	Moderate
	Bathing Beach 2	Low
	Bathing Beach 3	Low
	Shilaoren	Moderate

## 5. Discussion

The beaches studied show varying vulnerability due to the difference in the geomorphic and hydroclimatic characteristics of the two regions. The factors responsible for the vulnerability of a beach to erosion can be complex, for example, the vulnerability assessment indicated that beaches in Zhejiang are more vulnerable to erosion from storm conditions. However, the storm conditions seem to be the primary source of beach materials here. During extreme storm events, cross-shore sediment processes affect the distribution of sediment on beaches<sup>[36]</sup>. In the Zhejiang region, the storm conditions played an important role in the distribution of sandy material on the beach. However, in Qingdao, the geology of the beaches and coastal engineering as well as fewer storm events have caused an increase in the resistance to erosion on the beaches.

## 5.1. Contributing factors during different stages

### 5.1.1. First stage

Storm conditions can exacerbate the susceptibility of a beach to erosion<sup>[10]</sup>. It could as well reduce the time required for a beach to recover from erosion under natural conditions. Usually, the beaches on the studied coasts have been regularly affected by typhoons. Between 1973 and 1998, the Chinese coast experienced several violent typhoon conditions. Although the coasts had only recorded catastrophic storm conditions after the 1980s. In particular, two historical typhoon events, Typhoon Polly in 1992 and Typhoon Winne in 1978 have caused serious impacts on the local economy and development of the Chinese coast. Typhoon Polly landed in Fujian Province on 31st August 1992, with a maximum wind speed of around 25 m/s and a central pressure of 975 hPa. It later moved northeast through the north of the Yellow Sea after entering Haizhou Wan on 1st September<sup>[5,40]</sup>. Similarly, Typhoon Winne landed at Wenling, Zhejiang Province with a maximum wind speed of 40 m/s and a central pressure of 960 hPa on 18th August 1997. It is one of the typhoons that made a land connection on the Chinese mainland. It crossed Zhejiang and Anhui provinces and entered Shandong Province. During these two typhoons, several tide stations in Qingdao exceeded the local warning tide level, which caused direct economic loss up to 680 million RMB and 271 million RMB, respectively<sup>[5]</sup>.

### 5.1.2. Second stage

It has been established that storm conditions can lead to beach area loss<sup>[10]</sup>. Up to 120 storm events have been recorded in Qingdao between 1898 and 1994<sup>[41]</sup>. Besides, extratropical storm surges occurred in Bohai Bay and Laizhou Bay in October 2003 and March 2007<sup>[29]</sup>. However, Zhejiang province of China is one of the locations that is mostly affected by storm conditions in China. The low-lying south Yangtze coastal plain has been reported to be vulnerable to coastal inundation since the middle Holocene<sup>[42]</sup>. Besides, there were a total of 6 obvious typhoon-level waves that occurred in the China sea in 2016 and 2017 with most of them having a strong influence on the Zhejiang coast<sup>[42]</sup>.

Naturally, all the beaches had a recurrent recovery from inundation during the second stage. Usually, beaches recover naturally after storm conditions<sup>[10]</sup>. However, the rate of recovery could be in the range of a few days to years depending on sediment supply by catchment rivers, longshore transport energy, the type of wave on the beach as well as the energy condition of the waves<sup>[3,4]</sup>. The nearshore conditions on Qingdao beaches do not support sedimentation and the major recovery source of sediment to the lost beach is sand nourishment<sup>[12]</sup>. The sandy beaches in Qingdao have been affected by shortage of sediment due to sand dredging on the beaches and/or adjacent offshore areas and reduction in the sand sourced from river channels and longshore transport. Similarly, the natural condition on Zhejiang beaches supports the sedimentation of muddy materials, however, the harsh condition of the coast could have improved the presence of sandy material on the studied beaches<sup>[18,30]</sup>.

### 5.1.3. Third stage

In Zhejiang, the shoreline recovery has followed a natural trend with all of the beaches here recording the progression of seaward movement (**Figures 2 and 3**). Although the studied beaches did show evidence of increased human activities including minor coastal modification.

However, the seaward movement here during this stage cannot be connected to human activity such as beach nourishment procedures since there have not been any substantial beach management procedures on sandy beaches in Zhejiang.

## 5.2. Contributing factors for the long-term shoreline change of beach on the different coasts

Factors affecting accretion or deposition on embayed sandy beaches on rocky headlands include the nearshore wave characteristic, tidal current, storm conditions, longshore transport, local geology, and the

anthropogenic activities occurring on respective beaches<sup>[3,4,19–23]</sup>. Despite the beaches having different local geological characteristics, the trend of change on the coast is similar. Inferable, natural hydro physical conditions, in particular, wave and storm conditions have contributed to the loss in beach volume in the two study locations. Considering the low-lying sea level of these coasts, waves and storm conditions are one of the most destructive natural disasters that will affect the inundation recorded. Besides, due to the nearshore properties (including beach slope) of the studied beaches, sea level rise could affect the storm conditions in Zhejiang<sup>[38]</sup> and Qingdao<sup>[5,43]</sup> coasts. For example, in the long term, the result of this analysis shows a positive correlation between the effect of Sea level rise and storm surge (**Figures 4 and 5**). The contemporary increase in Sea-level results from Kanmen and Yantai Sea-level measuring stations have indicated a positive correlation with the frequency of observed storm surge events on the beaches of Zhejiang and Qingdao.

The intensity and frequency of storm conditions on Qingdao and Zhejiang beaches are different, with Zhejiang beaches being more open to frequent attacks of high intensity. Eventually, beaches are expected to recover after storm event<sup>[10]</sup>, but the source of sediment supply to Qingdao and Zhejiang beaches can either be natural (longshore transported from river catchments or offshore origin) or human-aided (sand nourishment). Overall, the intensity of human modification and nearshore hydrodynamics has culminated in the recoveries on these beaches, with the effect more evident on Qingdao beaches. The next subsections describe these factors in detail for each location.

### **5.2.1. Muddy coast beaches (Zhejiang) controlling factors**

The effect of storm conditions on Zhejiang beaches has been established<sup>[5,40,42]</sup>. However, the pathway to the recovery of studied Zhejiang beaches from the storm condition is not the same as those in Qingdao. The studied beaches are located in a muddy coastal environment that hardly receives sediment supply from the catchment Yangtze River. And the Yangtze is the primary source of sediment supply to the Zhejiang region, however, close to 80% of its suspended transports are deposited in the coastal shelf of the East China Sea<sup>[7,31]</sup>. Moreover, several authors have concluded that the Three Gorges Dam which was constructed in 2003 has trapped up to 60% of Yangtze River suspended transport, reducing the amount of possible sedimentation of the coast<sup>[2,14]</sup>. Ultimately, the nearshore conditions of the coast do not favor the deposition of sandy materials. Although the Taiwan Warm Current pushes fine sediment towards Sanmen bay to be deposited in adjacent beaches creating a muddy coast around the studied sandy beaches. But still, the sedimentation rate is nearly zero as the suspended material approaches the coast leading to low sedimentation and hence does not favor the natural recovery of the beaches and the beach sediment is not replenished as fast as storm conditions remove them.

In an interesting twist, the storm condition on the studied beach has been linked to the presence of sand material on a coast characterized by low-energy swells<sup>[18,30]</sup>. The high waves created during the storm conditions, the topography, and the morphology of the beaches could promote the sedimentation of sand material by shifting the Sand Mud Transition (SMT) offshore. Moreover, the embayment condition of the beaches has promoted sand deposition during storm conditions<sup>[18]</sup>. Besides, Anthony et al. and Dolique and Anthony<sup>[16,17]</sup> have reported that the distribution of sandy material to small, embayed beaches on mud banks is primarily affected by wave intensity on the coast. Since the storm conditions on this coast are frequent<sup>[30]</sup>, the high waves generated during storm conditions transport sand materials to the beaches, creating sandy beach pockets in a muddy coastal environment.

### **5.2.2. Sandy coast beaches (Qingdao) controlling factors**

Qingdao is affected by weather events such as typhoons and heavy rain that can lead to disaster throughout the year, especially when crossing typhoons combined with wind, storms, and tides<sup>[5,29]</sup>. Besides, the natural supply of sediment to the beaches in Qingdao has been inconsistent since the 1950s and hence has been eroding

due to the shortage in the sediment supply via alongshore drift and sand dredging from the beach and offshore. The sediment load delivered from the Yellow River to the Bohai Sea has decreased sharply from  $1.08 \times 10^9$  t/y in the 1950s to  $0.15 \times 10^9$  t/y from 2000 to 2005<sup>[12]</sup>. Also, evidence of shoreline erosion was reported in Qingdao in 2013 and 2017 as an aftermath of a storm condition. There has been extensive removal of sand from beaches and offshore shallow waters in Qingdao since the 1980s. This sand removal has been linked to the erosion features on the coast up till the 20th century. This had led to the recent coastal engineering remediation procedures including the seawall at Bathing Beach 2 (**Figure 2(g)**). However, strict laws by the Chinese government have further prevented the excavation of beach sand in Qingdao. The beaches have received recurrent sediment nourishment projects in recent years too. This remediation put in place has compensated for the deficiency in the sediment supplied to the beaches and hence has stabilized the shoreline position.

## 6. Conclusion

We examine the implication of storm conditions and anthropogenic activities on the shoreline position of 4 sandy beaches in Qingdao and 4 sandy beaches in the Zhejiang regions of China. Ultimately, we contrast the factors responsible for the shoreline change in different geomorphic environments and evaluate the presence of Sandy beach in a muddy coastal environment.

The research has revealed that the sandy beaches in Zhejiang are more vulnerable to erosion than those in Qingdao. In addition, the sandy beaches in both regions have been eroding since the early 1970s. During the first stage, both types of beaches experienced serious erosion as a response to severe storm conditions that dominated the period. During the second stage, the beaches initially recovered as a natural process, however, they were again eroded after 2015 as a result of suspected hydroclimatic conditions. During the third stage, the beaches recorded accretion. Coastal protection and beach nourishment activities have contributed significantly to this advancement. Overall, this research has linked the landward beach regression to a combination of the shortage of sediment supply and storm conditions in Qingdao. Although the beach protection and sand nourishment procedures have improved recently in Qingdao, this has removed the earlier harsh conditions on the beach, however, erosion is still persistent except on Bathing Beach 2. In Zhejiang, the sandy beaches have been constantly shaped by the storm condition of the coast. Even though erosion is still persistent here, the storm condition is the main factor that promotes the supply of the beaches with sand material.

The constant negative trend recorded is an indication of the bigger picture happening around the world. Sandy coastlines around the world are currently being eroded at an alarming rate. Low-lying beaches have been constantly affected by human activities concomitantly with the nearshore hydroclimate regime. These actions have been persistent around the world and happening at different scales. The “non-severity” could cause the constant neglect of these beaches and continuous exposure to the contemporary increasing pressures including climate change and human pressure including exploitation of beach minerals such as beach sand. This situation could lead to irreversible problems when the beaches reach a tipping point if better management plans are not implemented.

## Author contributions

Conceptualization, AJO, and YHW; methodology, AJO, YHW, and NAHM; formal analysis, AJO; data curation, AJO; writing—original draft preparation, AJO; writing—review and editing, AJO, YHW, YH, and SA; visualization, AJO; supervision, YHW; project administration, YHW; funding acquisition, YHW, and NAHM. All authors have read and agreed to the published version of the manuscript.

## Acknowledgments

This research was funded jointly by the Special Survey of Basic Scientific and Technological Resources (2022FY202402), the Shandong Provincial Natural Science Foundation, China (ZR2022MD109), the General Program of National Natural Science Foundation of China (42376163), Joint funds of the National Natural Science Foundation of China (U2306218), and National Key Research and Development Program (2016YFC0402602).

## Conflict of interest

The authors declare that they have no known competing financial interests or personal relationships that could have appeared to influence the work reported in this paper.

## References

1. Cai F, Cao C, Qi H, et al. Rapid migration of mainland China's coastal erosion vulnerability due to anthropogenic changes. *Journal of Environmental Management* 2022; 319: 115632. doi: 10.1016/j.jenvman.2022.115632
2. Xu G, Liu J, Liu S, et al. Modern muddy deposit along the Zhejiang coast in the East China Sea: Response to large-scale human projects. *Continental Shelf Research* 2016; 130: 68–78. doi: 10.1016/j.csr.2016.10.007
3. Bellido C, Anfuso G, Plomaritis TA, Rangel-Buitrago N. Morphodynamic behaviour, disturbance depth and longshore transport at Camposoto Beach (Cadiz, SW Spain). *Journal of Coastal Research* 2011; 35–39.
4. Dodet G, Castelle B, Masselink G, et al. Beach recovery from extreme storm activity during the 2013–14 winter along the Atlantic coast of Europe. *Earth Surface Processes and Landforms* 2019; 44(1): 393–401. doi: 10.1002/esp.4500
5. Ma Y, Wu Y, Shao Z, et al. Impacts of sea level rise and typhoon intensity on storm surges and waves around the coastal area of Qingdao. *Ocean Engineering* 2022; 249: 110953. doi: 10.1016/j.oceaneng.2022.110953
6. Chen Z, Huang P, Huang H, et al. Characteristics of modern sedimentation in Qingdao bays. *Chinese Journal of Oceanology and Limnology* 2009; 27: 683–696. doi: 10.1007/s00343-009-9124-0
7. Liang J, Liu J, Xu G, Chen B. Grain-size characteristics and net transport patterns of surficial sediments in the Zhejiang nearshore area, East China Sea. *Oceanologia* 2020; 62(1): 12–22. doi: 10.1016/j.oceano.2019.06.002
8. Osanyintuyi AJ, Wang YH, Mokhtar NAH. Nearly five decades of changing shoreline mobility along the densely developed Lagos barrier-lagoon coast of Nigeria: A remote sensing approach. *Journal of African Earth Sciences* 2022; 194: 104628. doi: 10.1016/j.jafrearsci.2022.104628
9. Warnasuriya TWS, Kumara MP, Gunasekara SS, et al. An improved method to detect shoreline changes in small-scale beaches using google earth pro. *Marine Geodesy* 2020; 43(6): 541–572. doi: 10.1080/01490419.2020.1822478
10. Cai F, Su X, Liu J, et al. Coastal erosion in China under the condition of global climate change and measures for its prevention. *Progress in Natural Science* 2009; 19(4): 415–426. doi: 10.1016/j.pnsc.2008.05.034
11. Qiao G, Mi H, Wang W, et al. 55-year (1960–2015) spatiotemporal shoreline change analysis using historical DISP and Landsat time series data in Shanghai. *International Journal of Applied Earth Observation and Geoinformation* 2018; 68: 238–251. doi: 10.1016/j.jag.2018.02.009
12. Yin P, Duan X, Gao F, et al. Coastal erosion in Shandong of China: Status and protection challenges. *China Geology* 2018; 1(4): 512–521. doi: 10.31035/cg2018073
13. Kirby R. Chapter four: Distinguishing accretion from erosion-dominated muddy coasts. In: Healy T, Wang Y, Healy JA (editors). *Muddy Coasts of the World: Processes, Deposits and Function (Proceedings in Marine Science)*. Elsevier Science; 2002; Volume 4. pp. 61–81. doi: 10.1016/S1568-2692(02)80078-X
14. Jia J, Zhang X, Zhou R, et al. Sources of sediment in tidal flats off Zhejiang coast, southeast China. *Journal of Oceanology and Limnology* 2021; 39: 1245–1255. doi: 10.1007/S00343-020-0179-2
15. Gardel A, Anthony EJ, Dos Santos VF, et al. Fluvial sand, Amazon mud, and sediment accommodation in the tropical Maroni River estuary: Controls on the transition from estuary to delta and chenier plain. *Regional Studies in Marine Science* 2021; 41: 101548. doi: 10.1016/j.rsma.2020.101548
16. Anthony EJ, Gardel A, Dolique F, et al. Mud banks, sand flux and beach morphodynamics: Montjoly Lagoon Beach, French Guiana. In: Maanan M, Robin M (editors). *Sediment Fluxes in Coastal Areas*. Springer, Dordrecht; 2015. pp. 75–90. doi: 10.1007/978-94-017-9260-8\_4
17. Dolique F, Anthony EJ. Short-term profile changes of sandy pocket beaches affected by Amazon-derived mud, Cayenne, French Guiana. *Journal of Coastal Research* 2005; 21(6(216)): 1195–1202. doi: 10.2112/04-0297.1
18. Guo J, Shi L, Chen S, et al. Sand-mud transition dynamics at embayed beaches during a typhoon season in eastern China. *Marine Geology* 2021; 441: 106633. doi: 10.1016/j.margeo.2021.106633
19. King EV, Conley DC, Masselink G, et al. Wave, tide and topographical controls on headland sand bypassing.

- Journal of Geophysical Research: Oceans* 2021; 126(8): e2020JC017053. doi: 10.1029/2020JC017053
20. Schiaffino CF, Brignone M, Ferrari M. Application of the parabolic bay shape equation to sand and gravel beaches on Mediterranean coasts. *Coastal Engineering* 2012; 59(1): 57–63. doi: 10.1016/j.coastaleng.2011.07.007
  21. Robinet A, Castelle B, Idier D, et al. Controls of local geology and cross-shore/longshore processes on embayed beach shoreline variability. *Marine Geology* 2020; 422: 106118. doi: 10.1016/j.margeo.2020.106118
  22. Do K, Yoo J. Morphological response to storms in an embayed beach having limited sediment thickness. *Estuarine, Coastal and Shelf Science* 2020; 234: 106636. doi: 10.1016/j.ecss.2020.106636
  23. Fellowes TE, Vila-Concejo A, Gallop SL, et al. Wave shadow zones as a primary control of storm erosion and recovery on embayed beaches. *Geomorphology* 2022; 399: 108072. doi: 10.1016/j.geomorph.2021.108072
  24. da Silveira YG, Bonetti J. Assessment of the physical vulnerability to erosion and flooding in a sheltered coastal sector: Florianópolis Bay, Brazil. *Journal of Coastal Conservation* 2019; 23: 303–314. doi: 10.1007/s11852-018-0659-0
  25. de Andrade TS, de Oliveira Sousa PHG, Siegle E. Vulnerability to beach erosion based on a coastal processes approach. *Applied Geography* 2019; 102: 12–19. doi: 10.1016/j.apgeog.2018.11.003
  26. Ding D, Yang J, Li G, et al. A geomorphological response of beaches to Typhoon Meari in the eastern Shandong Peninsula in China. *Acta Oceanologica Sinica* 2015; 34: 126–135. doi: 10.1007/s13131-015-0644-5
  27. Irham M, Rusydi I, Haridhi HA, et al. Coastal vulnerability of the west coast of Aceh Besar: A coastal morphology assessment. *Journal of Marine Science and Engineering* 2021; 9(8): 815. doi: 10.3390/jmse9080815
  28. Rehman S, Jahangir S, Azhoni A. GIS based coastal vulnerability assessment and adaptation barriers to coastal regulations in Dakshina Kannada district, India. *Regional Studies in Marine Science* 2022; 55: 102509. doi: 10.1016/j.rsma.2022.102509
  29. Wang N, Hou Y, Mo D, Li J. Hazard assessment of storm surges and concomitant waves in Shandong Peninsula based on long-term numerical simulations. *Ocean & Coastal Management* 2021; 213: 105888. doi: 10.1016/j.ocecoaman.2021.105888
  30. Fan D, Li C, Wang P. Influences of storm erosion and deposition on rhythmites of the Upper Wenchang Formation (Upper Ordovician) around Tonglu, Zhejiang Province, China. *Journal of Sedimentary Research* 2004; 74(4): 527–536. doi: 10.1306/010304740527
  31. Wang Y, Zhu D, Wu X. Chapter thirteen: Tidal flats and associated muddy coast of China. In: Healy T, Wang Y, Healy JA (editors). *Muddy Coasts of the World: Processes, Deposits and Function (Proceedings in Marine Science)*. Elsevier Science; 2002; Volume 4. pp. 319–345. doi: 10.1016/S1568-2692(02)80087-0
  32. Zhou Y, Ye Q, Shi W, et al. Wave characteristics in the nearshore waters of Sanmen Bay. *Applied Ocean Research* 2020; 101: 102236. doi: 10.1016/j.apor.2020.102236
  33. GloVis. Available online: <http://glovis.usgs.gov/>.
  34. Zhou Y, Wang F, Zhang J, et al. Investigation of waves in Sanmen Bay during typhoons and their influence on moored vessels. *Ocean Dynamics* 2022; 72: 443–454. doi: 10.1007/s10236-022-01513-z
  35. Alexandrakakis G, Poulos SE. An holistic approach to beach erosion vulnerability assessment. *Scientific Reports* 2014; 4: 6078. doi: 10.1038/srep06078
  36. Vandarakis D, Panagiotopoulos IP, Loukaidi V, et al. Assessment of the coastal vulnerability to the ongoing sea level rise for the exquisite Rhodes Island (SE Aegean Sea, Greece). *Water* 2021; 13(16): 2169. doi: 10.3390/w13162169
  37. Ministry of Natural Resources of People’s Republic China. 2021 China sea level bulletin (Chinese version). Available online: [http://gi.mnr.gov.cn/202205/t20220507\\_2735509.html](http://gi.mnr.gov.cn/202205/t20220507_2735509.html) (accessed on 6 November 2022).
  38. Fang Y, Yin J, Wu B. Flooding risk assessment of coastal tourist attractions affected by sea level rise and storm surge: A case study in Zhejiang Province, China. *Natural Hazards* 2016; 84: 611–624. doi: 10.1007/s11069-016-2444-4
  39. Ministry of Natural Resources of People’s Republic China. China marine disaster bulletin (Chinese version). Available online: <https://www.mnr.gov.cn/sj/sjfw/hy/gbgb/zghyzhgb/index.html> (accessed on 9 November 2022).
  40. Dong S, Gan B, Hao X. Selection of environmental conditions for nearshore structure design. *Journal of Ocean University of China* 2004; 3: 111–114. doi: 10.1007/s11802-004-0019-6
  41. Wang L, Chen B, Zhang J, Chen Z. A new model for calculating the design wave height in typhoon-affected sea areas. *Natural Hazards* 2013; 67: 129–143. doi: 10.1007/s11069-012-0266-6
  42. Wang S, Ge J, Kilbourne KH, Wang Z. Numerical simulation of mid-Holocene tidal regime and storm-tide inundation in the south Yangtze coastal plain, East China. *Marine Geology* 2020; 423: 106134. doi: 10.1016/j.margeo.2020.106134
  43. Feng J, Jiang W, Bian C. Numerical prediction of storm surge in the Qingdao area under the impact of climate change. *Journal of Ocean University of China* 2014; 13: 539–551. doi: 10.1007/s11802-014-2222-4